

Document downloaded from:

<http://hdl.handle.net/10251/165283>

This paper must be cited as:

Vallés-García, C.; Cabrero-Antonino, M.; Navalón Oltra, S.; Alvaro Rodríguez, MM.; Dhakshinamoorthy, A.; García Gómez, H. (2020). Nitro functionalized chromium terephthalate metal-organic framework as multifunctional solid acid for the synthesis of benzimidazoles. *Journal of Colloid and Interface Science*. 560:885-893.  
<https://doi.org/10.1016/j.jcis.2019.10.093>



The final publication is available at

<https://doi.org/10.1016/j.jcis.2019.10.093>

Copyright Elsevier

Additional Information

# **Nitro functionalized chromium terephthalate metal-organic framework as multifunctional solid acid for the synthesis of benzimidazoles.**

Cristina Vallés-García,<sup>a</sup> María Cabrero-Antonino,<sup>a</sup> Sergio Navalón,<sup>\*,a</sup> Mercedes Álvaro,<sup>a</sup> Amarajothi Dhakshinamoorthy,<sup>\*,b</sup> Hermenegildo García<sup>\*,c,d</sup>

<sup>a</sup>Departamento de Química, Universitat Politècnica de València, C/Camino de Vera, s/n, 46022 Valencia, Spain

<sup>b</sup>School of Chemistry, Madurai Kamaraj University, Madurai-625 021, Tamil Nadu, India.

<sup>c</sup>Departamento de Química and Instituto Universitario de Tecnología Química (CSIC-UPV), Av. De los Naranjos s/n, 46022 Valencia, Spain.

<sup>d</sup>Center of Excellence for Advanced Materials Research, King Abdulaziz University, Jeddah, Saudi Arabia

## 4.1 Abstract

In the present work, nitro functionalized chromium terephthalate [MIL-101(Cr)-NO<sub>2</sub>] metal-organic framework is prepared and characterized by powder X-ray diffraction (XRD), elemental analysis, infrared spectroscopy (IR), X-ray photoelectron spectroscopy (XPS), scanning electron microscopy (SEM) and Brunauer–Emmett–Teller (BET) surface area. The inherent Lewis acidity of MIL-101(Cr)-NO<sub>2</sub> is confirmed by FT-IR spectroscopy using CD<sub>3</sub>CN as a probe molecule. The performance of MIL-101(Cr)-NO<sub>2</sub> as bifunctional catalyst (acid and redox) promoting the synthesis of wide range of benzimidazoles has been examined by catalyzed condensation on acid sites and subsequent oxidation dehydrogenation. The catalytic activity of MIL-101(Cr)-NO<sub>2</sub> is found to be superior than analogues catalysts like MIL-101(Cr)-SO<sub>3</sub>H, MIL-101(Cr)-NH<sub>2</sub>, UiO-66(Zr), UiO-66(Zr)-NO<sub>2</sub>, MIL-100(Fe) and Cu<sub>3</sub>(BTC)<sub>2</sub> (BTC: 1,3,5-Benzenetricarboxylate) under identical reaction conditions. The structural stability of MIL-101(Cr)-NO<sub>2</sub> is supported by leaching analysis and reusability tests. MIL-101(Cr)-NO<sub>2</sub> solid is used five times without decay in its activity. Comparison of the fresh and five times used MIL-101(Cr)-NO<sub>2</sub> solids by powder XRD, SEM and elemental analysis indicate identical crystallinity, morphology and the absence of chromium leaching, respectively.

## 4.2 Introduccion

Metal organic frameworks (MOFs) are crystalline porous materials whose crystal structure is assembled by the coordination of metal ions or clusters with rigid organic linkers defining one, two and three-dimensional structures. Since the discovery of MIL-101 (MIL: *Materiaux de l'Institute Lavoisier*) by Ferey and co-workers,<sup>1</sup> this solid has been extensively used as Lewis acid for wide range of organic reactions<sup>2-6</sup> including acetalization, condensation, oxidation, CO<sub>2</sub> fixation and coupling reactions due to its robust stability.<sup>7, 8</sup> The catalytic activity derives from the presence of coordinatively unsaturated metal centres around Cr<sup>3+</sup> ions upon removal of solvent molecules by thermal activation and its robust structure. Furthermore, isostructural MIL-101 MOFs were also prepared by replacing terephthalic acid present in the parent MIL-101 by 2-aminothephtalic acid or 2-hydroxysulfonylterephthalic acid, among others, to obtain MIL-101(Cr)-NH<sub>2</sub> or MIL-101(Cr)-SO<sub>3</sub>H, respectively. The activity of MIL-101(Cr)-NH<sub>2</sub> and MIL-101(Cr)-SO<sub>3</sub>H has been studied in base catalyzed reactions including Knoevenagel condensation<sup>9-14</sup> and Brønsted acid catalyzed reactions<sup>15-17</sup>, respectively. Besides introducing active sites on the ligand, the Lewis acidity around Cr<sup>3+</sup> can also be enhanced by electron withdrawing substituents on the linker, thus, increasing the catalytic performance of MIL-101(Cr)-H<sup>18</sup>. Hence, compared to MIL-101(Cr)-H, MIL-101(Cr)-NO<sub>2</sub> has shown improved activity in the oxidative coupling of benzyl amine<sup>18</sup> and acetalization of benzaldehyde.<sup>19</sup> However, the number

of examples determining the promotional effect in the catalytic activity of MIL-101(Cr)-H due to the presence of NO<sub>2</sub> is still limited.

Many biologically relevant compounds, natural products and drug molecules contain benzimidazole<sup>20, 21</sup> as a common core unit and hence considerable efforts have been made to develop new and efficient methods for the synthesis of benzimidazole and its derivatives. Benzimidazoles have been synthesised through the reaction between benzaldehydes and *o*-phenylenediamine, either with homogeneous or heterogeneous catalysts which include sulfamic acid,<sup>22</sup> FeCl<sub>3</sub>·6H<sub>2</sub>O,<sup>23</sup> In(OTf)<sub>3</sub>,<sup>24</sup> Sc(OTf)<sub>3</sub>,<sup>25</sup> ionic liquids,<sup>26</sup> iodine,<sup>27</sup> activated carbon,<sup>28</sup> clayzic,<sup>29</sup> and FeCl<sub>3</sub>/Al<sub>2</sub>O<sub>3</sub>.<sup>30</sup> On other hand, benzimidazole has also been synthesised by a series of MOFs as heterogeneous catalysts with different active centres. For example, a zinc-based MOF was reported to promote the condensation of aldehyde with diamines to obtain benzimidazoles.<sup>31</sup> I<sub>2</sub>@Cd-MOF was used as heterogeneous catalyst to perform the condensation of aldehydes and amines to give benzimidazoles.<sup>32</sup> On other hand, UiO-66(Zr)-NH<sub>2</sub>SO<sub>3</sub>H (UiO: University of Oslo) was reported as a heterogeneous Brønsted acid catalyst for the synthesis of benzimidazole derivatives.<sup>33</sup> In another report, UiO-66(Zr)-NH<sub>2</sub>-TC-Cu (TC: thiophene-2-carbaldehyde) was employed as solid catalyst for the synthesis of various benzimidazoles.<sup>34</sup> These catalysts require post-synthetic modification of the as-synthesised material to install the active sites while such post-synthetic treatment is not required in the present work.

MOFs comprising Lewis acid metal nodes as part of a highly porous lattice are currently under investigation as solid catalysts.<sup>35-37</sup> One of the current interests in heterogeneous catalysis by MOFs is to show the ability of these materials to act as multifunctional catalysts promoting reactions in where the reaction mechanism requires more than one type of active site.<sup>38-44</sup> Multifunctionality in MOFs can arise from the activity of transition metal centers as Lewis acid as well as their ability to act as oxidation centers to promote oxidation reactions.<sup>41</sup> In a previous study, we have shown that MOFs can promote aerobic oxidations by activation of molecular oxygen and generation of hydroperoxyl and other reactive oxygen species.<sup>45-49</sup> Moreover it has been shown that the catalytic activity to promote aerobic oxidations is also strongly influenced by the presence of substituents on the linker. Inductive effects can increase the electronegativity of the linker and, as consequence, the oxidation potential of the nodal metal cation.<sup>18, 50</sup>

In the present study two robust MOF solids are used to demonstrate the bifunctional catalytic activity. These MOFs were selected based on their catalytic and structural stability. Specifically herein we have used MIL-101 both of the Cr and Fe forms and UiO-66(Zr) as solid catalysts due to their high stability. Both MOFs have in common terephthalic acid as organic linker and for both types of structures preparation of isostructural materials with organic substituents in the terephthalic acid has been reported in the literature.<sup>18</sup> Other common points between these two MOFs are their large specific BET surface area and their high porosity that allow easy

diffusion of the reagents and products within the internal pores. Therefore, the catalytic performance of a series of MOFs like MIL-101(Cr)-H, MIL-101(Cr)-NO<sub>2</sub>, MIL-101(Cr)-SO<sub>3</sub>H, MIL-101(Cr)-NH<sub>2</sub>, UiO-66(Zr), UiO-66(Zr)-NO<sub>2</sub>, MIL-100(Fe) and Cu<sub>3</sub>(BTC)<sub>2</sub> is studied in the cyclocondensation between benzaldehyde and *o*-phenylenediamine to achieve 2-phenylbenzimidazole involving Lewis and redox active sites.

## 4.3 Experimental

### 4.3.1 Materials

All the reagents, solvents were purchased from Sigma-Aldrich with analytical or HPLC grade and used as received.

### 4.3.2 Catalyst preparation

MIL-101(Cr)-X (X: H, NO<sub>2</sub>, NH<sub>2</sub>, SO<sub>3</sub>H) solids have been prepared according to previous reports.<sup>1, 51</sup> Briefly, the corresponding amount (1.5 mmol) of terephthalic acid or 2-nitroterephthalic acid and Cr(NO<sub>3</sub>)<sub>3</sub>·9H<sub>2</sub>O (for the synthesis of MIL-101(Cr)-H) or CrCl<sub>3</sub> (for the synthesis of MIL-101(Cr)-NO<sub>2</sub>) (1 mmol) were introduced into a Teflon autoclave containing demineralized water (8 mL). Then, HF (10 μL) was added for the synthesis of MIL-101(Cr)-H. The autoclave was closed and heated at 200 °C for 8 h or 180 °C for 120 h for the preparation of MIL-101(Cr)-H and MIL-101(Cr)-NO<sub>2</sub>, respectively. Then, the autoclave was cooled down to room temperature and the

obtained solid was washed two consecutive times using dimethylformamide (DMF, 120 °C for 1 h) and, then, three consecutive times with ethanol (80 °C) both under continuous magnetic stirring. MIL-101(Cr)-NH<sub>2</sub> was prepared by the post-synthetic reduction of the nitro groups present in preformed MIL-101(Cr)-NO<sub>2</sub> solid with SnCl<sub>2</sub>·H<sub>2</sub>O according to previous reports.<sup>18, 52</sup> Further, MIL-101(Cr)-SO<sub>3</sub>H was obtained by post-synthetic sulfonation of the parent MIL-101(Cr)-H with chlorosulfonic acid as previously reported.<sup>18, 53</sup> These resulting solids were dried in an oven at 100 °C for 24 h.

UiO-66(Zr)-X (X: H or NO<sub>2</sub>) solids have been prepared by adopting previously reported procedures.<sup>48, 54</sup> Briefly, terephthalic acid or 2-nitroterephthalic acid (1 mmol) and ZrCl<sub>4</sub> (1 mmol) were added to a Teflon autoclave containing DMF (3 mL). The autoclave was closed and heated at 220 °C for 12 or 24 h for the preparation of UiO-66(Zr) and UiO-66(Zr)-NO<sub>2</sub>, respectively. Once the autoclave was cooled to room temperature by standing at the ambient, the resulting solids were collected and washed with DMF at 60 °C for 1 h. Then, the solids were submitted to Soxhlet extraction using methanol as solvent for 12 h. The resulting solids were dried in an oven at 100 °C for 24 h.

### **4.3.3 Catalyst characterization**

Powder XRD of MIL-101(Cr)-X (X: H, NO<sub>2</sub>, NH<sub>2</sub>, SO<sub>3</sub>H) and UiO-66(Zr)-X (X: H or NO<sub>2</sub>) were recorded using a Philips XPert



diffractometer equipped with a graphite monochromator (40 kV and 45 mA) employing Ni-filtered CuK $\alpha$  radiation. ATR-FTIR spectra of the MIL-101(Cr)-X and UiO-66(Zr)-X series were measured with a Bruker Tensor 27 instrument. Prior to ATR-FTIR measurements the solid samples were dried in an oven at 100 °C for 16 h to remove physisorbed water. X-ray photoelectron spectra (XPS) of the solids prepared were collected on a SPECS spectrometer with a MCD-9 detector using a monochromatic Al (K $\alpha$ = 1486.6 eV) X-ray source. Spectra deconvolution was performed with CASA software using the C 1s peak at 284.4 eV as binding energy reference. Isothermal nitrogen adsorption measurements were collected at 77 K using a Micromeritics ASAP 2010 apparatus. The metal content of the MOFs was determined by inductively coupled plasma-atomic emission spectroscopy (ICP-AES). The solid MOF samples were digested in concentrated HNO<sub>3</sub> (15 mL, 80 °C, 24 h) prior to ICP-AES analyses. Thermogravimetric analyses (TGA) were measured on a TGA/SDTA851e Mettler Toledo station. SEM images were captured using a Zeiss instrument.

#### **4.3.4 Reaction procedure**

In a typical reaction procedure, 1,2-benzenediamine (**1**, 0.5 mmol) and benzaldehyde (**2**, 0.55 mmol) were dissolved in 2 mL of solvent. To this solution 30 mg (0.1 mmol of Cr) MIL-101(Cr)-NO<sub>2</sub> catalyst was added. The catalyst loading of other tested catalysts was 0.1 mmol of metal. This suspension was placed in hot plate preheated at 70 °C. The progress of the reaction was monitored by gas chromatography

by sampling periodically aliquots of the reaction mixture using known amounts of nitrobenzene as internal standard. The conversion of **2** and the selectivity of the final product were determined by gas chromatography using calibration plots. Product identity was confirmed by GC-MS and  $^1\text{H-NMR}$  spectroscopy.

Hot-filtration experiment was performed following the typical reaction procedure as described above. However, the catalyst was filtered after 10 min reaction time and the reaction mixture without solid was allowed to react further for the remaining time. Also, the course of the reaction was followed as indicated above determining the reaction mixture at identical time intervals as in the case when the MOF was not filtered. Kinetic plots with and without solid catalyst were compared.

Reusability experiments were performed following the typical reaction procedure as described above. After the reaction time, the catalyst was recovered by filtration and repeatedly washed with acetonitrile and dried at 100 °C in an oven for 24 h. Then, this used catalyst was employed for subsequent runs with fresh reactants and solvents.

## **4.4 Results and discussion**

### **4.4.1 Structural description of catalysts**

MIL-101(Cr)-H and its isostructural materials were prepared following earlier reported procedures.<sup>1, 18, 51</sup> Powder XRD confirms that the MIL-101(Cr)-X (X: H, NO<sub>2</sub>, NH<sub>2</sub> and SO<sub>3</sub>H) are isostructural with the parent MIL-101(Cr)-H (Fig. 1). FT-IR spectroscopy shows the presence of the corresponding functional groups on the terephthalate ligand by providing their characteristic vibrations peaks (Fig. S1-S4). The chromium metal content was determined by ICP-AES of previously digested MIL-101(Cr)-X samples and the values are in good agreement with the theoretical formula of these MOFs (Table 1). Isothermal nitrogen adsorption measurements confirm the high surface area and pore volume of the parent MIL-101(Cr)-H solid. The presence of functional groups on the terephthalate linker decreases these values reflecting the space occupied by the substituents. Thermogravimetric analysis of MIL-101(Cr)-H and MIL-101(Cr)-NO<sub>2</sub> are provided in Fig. S5. No significant differences in thermal stability were observed for both materials. XPS of the MIL-101(Cr)-X (X: H, NO<sub>2</sub>, SO<sub>3</sub>H and NH<sub>2</sub>) solids confirms the presence and types of the individual atoms expected for the corresponding MOF (C1s, O1s, Cr, N or S) in agreement with previous reports (Fig. S6-S9).<sup>48</sup> Specifically, it shows the presence of two individual components attributed to the aromatic carbons at 284.6 eV and carboxylate groups at 288.06 eV. The experimental O 1s peak contains in some cases a single component attributed to the carboxylate groups. All the samples also present a single component for Cr based on the Cr 2p peak with only very minor shift in the binding energy. In contrast, the position of the N 1s peak in MIL-101(Cr)-NH<sub>2</sub> compared to that of MIL-101(Cr)-NO<sub>2</sub> undergoes a remarkable change in binding energy from 395.0 to

405.5 eV, respectively. Similar to powder XRD (Fig. 1), metal content determination by ICP-AES (Table 1), isothermal nitrogen adsorption (Table 1) and XPS also support the successful preparation of UiO-66(Zr) and UiO-66(Zr)-NO<sub>2</sub> samples (Fig. S10-S11).<sup>48</sup>

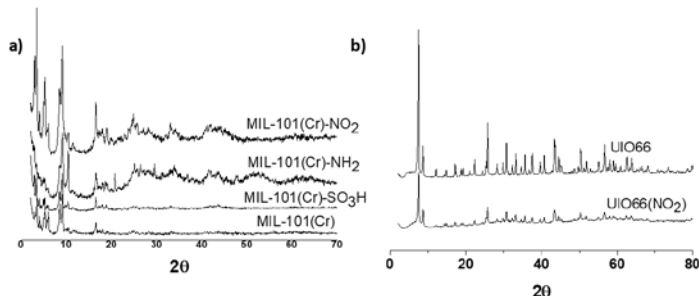


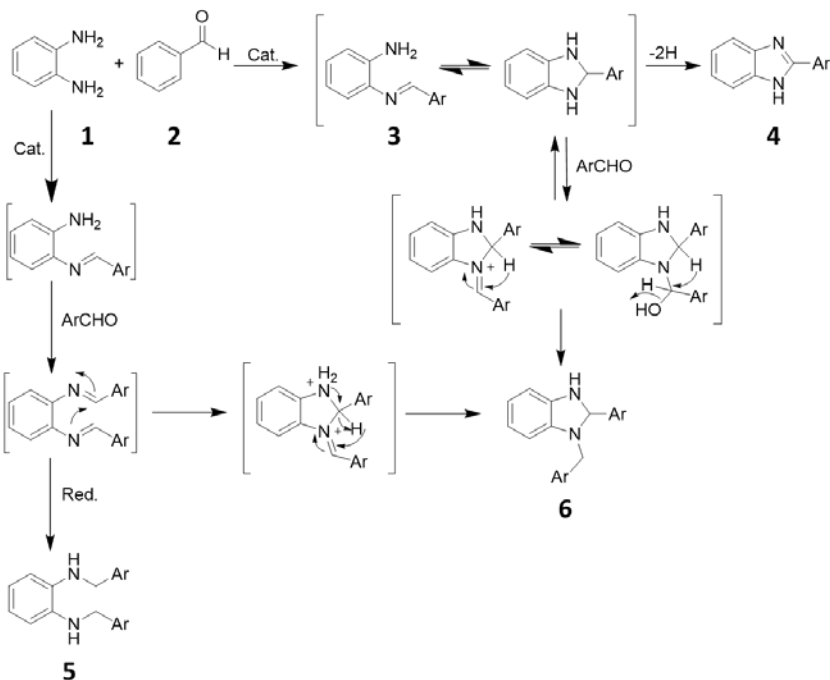
**Fig. 1** Powder XRD of (a) MIL-101(Cr)-X and (b) UiO-66(Zr)-X solids.

**Table 1** List of MOFs employed as catalysts in this work together with some relevant textural and analytical data.

Entry	Catalyst	BET Surface area (m <sup>2</sup> g <sup>-1</sup> )	Pore volume (cm <sup>3</sup> g <sup>-1</sup> )	Theoretical metal content (%) / Calculated by ICP (%)
1	MIL-101(Cr)-H {Cr <sub>3</sub> F(H <sub>2</sub> O) <sub>2</sub> O(BDC) <sub>3</sub> }	2740	2.20	21.77 / 22.84
2	MIL-101(Cr)-NO <sub>2</sub> {Cr <sub>3</sub> Cl(H <sub>2</sub> O) <sub>2</sub> O(BDC-NO <sub>2</sub> ) <sub>3</sub> }	1848	1.47	17.73 / 16.40
3	MIL-101(Cr)-SO <sub>3</sub> H {Cr <sub>3</sub> Cl(H <sub>2</sub> O) <sub>2</sub> O(BDC-SO <sub>3</sub> H) <sub>3</sub> }	1550	1.30	16.96 / 17.01
4	MIL-101(Cr)-NH <sub>2</sub> {Cr <sub>3</sub> Cl(H <sub>2</sub> O) <sub>2</sub> O(BDC-NH <sub>2</sub> ) <sub>3</sub> }	1555	1.15	20.97 / 21.50
5	UiO-66(Zr)	1258	0.73	32.80 / 34.70
6	UiO-66(Zr)-NO <sub>2</sub>	700	0.23	28.20 / 32.60
7	MIL-100(Fe) {Fe <sub>3</sub> F <sub>3</sub> O(BTC) <sub>3</sub> }	1205	0.55	23.00 / 22.20
8	Cu <sub>3</sub> (BTC) <sub>2</sub>	1250	0.57	31.20 / 32.40

#### 4.4.2 Catalytic activity

Aimed at demonstrating the influence of substituents on the activity of MOFs as bifunctional catalysts, the present study has focused on a model reaction of general interest in heterocyclic chemistry such as the cyclocondensation of *o*-phenyldiamine (**1**) with benzaldehyde (**2**) to form 2-phenylbenzimidazole (**4**). Benzimidazoles are nitrogenated heterocycles that find application as therapeutic agents and pharmaceutical compounds.<sup>55</sup> The reaction mechanism leading to the formation of the benzimidazole from **2** and **1** is well understood and comprises one step leading to the dihydrobenzimidazole that is catalyzed by acids and a subsequent step involving the oxidative dehydrogenation of the dihydrobenzimidazole intermediate resulting in the final heterocycle.<sup>56</sup> In those cases in where the oxidation step does not occur at a sufficient rate, formation of byproducts such as *N,N'*-dibenzylidenediimine (**5**) and 1-benzyl-2-phenyl-1H-benzimidazole (**6**) can be observed. Scheme 1 illustrates the elementary steps of the accepted reaction mechanism involved in the formation of the various products.



**Scheme 1** Elementary steps with indication of the nature of the catalytic site in the reaction pathway leading to **4** from **2** and **1** and by-products **5** and **6**.

According to the reaction mechanism shown in Scheme 1, a suitable catalyst for the cyclocondensation of **1** and **2** leading to **4** should be able to promote two elementary steps, the acid-catalyzed formation of 2-(benzylideneamino)aniline **3** and its oxidative aromatization towards **4**.<sup>56</sup> In principle imine formation does not require strong acid sites and can be promoted by acids of weak or medium acid strength. Regarding the oxidative step, although aromaticity of the ring is driving towards the final benzimidazole product, oxidation sites are required, particularly to avoid by-product formation. Considering that earlier results have shown the positive

influence of electron withdrawing groups on the linker on the catalytic activity, it can be expected that the same trend should be found here in the benzimidazole formation. The results presented below confirm the bifunctional activity of MOF in this cyclocondensation/oxidation showing the beneficial influence of nitro groups on the terephthalate linker to promote the oxidative steps in the mechanism.

The reaction of **1** with **2** to obtain **4** is typically catalyzed either by Lewis<sup>29, 57</sup> or Brönsted acids and redox centers.<sup>56, 58</sup> Initial attempts were made to synthesize these compounds using  $\text{Cu}_3(\text{BTC})_2$  MOFs, due to its intrinsic Lewis acid sites and redox activity of dimeric Cu metal centres. However, the chemical stability of  $\text{Cu}_3(\text{BTC})_2$  MOFs used for the condensation of **1** and **2** for benzimidazole synthesis is limited and the solid decomposes.<sup>59</sup> Hence, the present work aims to employ some of the structurally most robust MOFs as heterogeneous solid catalysts for the synthesis of benzimidazole. The results achieved are summarized in Table 2. The reaction of **1** and **2** in the presence of MIL-101(Cr)-H at room temperature afforded 32% yield of **4** at room temperature after 5 h (entry 1, Table 2). Under identical conditions, the use of MIL-101(Cr)-NO<sub>2</sub> afforded 42% yield (entry 2, Table 2). These results show the increase of activity for the synthesis of product **4** when using MIL-101(Cr)-NO<sub>2</sub> (TOF 0.38 h<sup>-1</sup>) respect to MIL-101(Cr)-H (TOF 0.21 h<sup>-1</sup>) working at room temperature. In a related work, Hamadi and co-workers also showed the benefits of using the heterogeneous UiO-66(Zr)-NH<sub>2</sub>SO<sub>3</sub>H solid as Brönsted acid catalyst respect to the parent UiO-66(Zr)-NH<sub>2</sub> for the preparation of

benzimidazole.<sup>33</sup> The reaction of **1** with **2** in the presence of MIL-101(Cr)-H and MIL-101(Cr)-NO<sub>2</sub> was carried out at 70 °C and the yields were 54 and 79%, respectively after 5 h (entries 3 and 5, Table 2). Then, the activity of MIL-101(Cr)-NO<sub>2</sub> was screened for the reaction between **1** and **2** under identical conditions in various solvents including acetonitrile/ethanol and toluene, observing 55 and 37% yields of **4**, respectively (entries 4 and 6 Table 2). The highest yield (82%) was achieved after 4 h in acetonitrile (entry 8, Table 2). It is likely that protic solvents such as ethanol interact strongly with the acid and basic sites, therefore decreasing the catalytic activity, while aromatic solvents may interact with the organic ligand and are typically strongly adsorbed in some MOF. A control experiment for the reaction of **1** and **2** under argon atmosphere resulted in a conversion of about 94% with around 10% yield of **4**. This result reinforces the need of oxygen to promote the oxidative dehydrogenation to form the imidazole ring. This oxidative dehydrogenation could involve either metal-oxygen adducts such as metaloxirane or metalo hydroperoxide and together with Lewis acidity required in the amino-carbonyl condensation, determines that MIL-101(Cr)-NO<sub>2</sub> acts as bifunctional (acid and redox) catalyst. In agreement with the role of oxygen as reagent to promote dehydrogenation, an additional control reaction was performed with similar conditions in the presence of pure oxygen atmosphere (Table 2, entry 20). A selectivity of 90% to **4** with 100% conversion of **1** (Fig. S12) was observed under pure oxygen atmosphere, thus reinforcing the role of the oxygen to promote imidazole formation as indicated in the Scheme 1. Table S1 summarizes the obtained turnover number



(TON) and turnover frequency (TOF) values for the series of catalysts tested in this work at 70 °C. SEM images comparing the morphology of MIL-101(Cr)-NO<sub>2</sub> before and after catalytic uses showed no significant differences suggesting catalyst stability (Fig. S13). Further, SEM images of the recovered after one use of MIL-101(Cr)-H, MIL-101(Cr)-NH<sub>2</sub>, MIL-101(Cr)-SO<sub>3</sub>H, MIL-100(Fe), UiO-66(Zr), UiO-66(Zr)-NO<sub>2</sub> and solids showed almost similar morphology compared to their respective fresh catalysts (Figs. S14-19) while Cu<sub>3</sub>(BTC)<sub>2</sub> indicated some change in its morphology (Fig. S20).

**Table 2** Summary of the catalytic results for the cyclocondensation of **1** and **2** to form **4** using MIL-101(Cr)-H and UiO-66(Zr)-based solid catalysts.<sup>a</sup>

Entry	Catalyst	Solvent	Time (h)	T (°C)	Conversion (%) <sup>b</sup>	Yield (%) <sup>b</sup>			
						<b>3</b>	<b>4</b>	<b>5</b>	<b>6</b>
1	MIL-101(Cr)-H	CH <sub>3</sub> CN	5	rt	72	4	32	36	28
2	MIL-101(Cr)-NO <sub>2</sub>	CH <sub>3</sub> CN	5	rt	79	7	42	24	27
3	MIL-101(Cr)-H	CH <sub>3</sub> CN	5	70	78	5	54	23	18
4	MIL-101(Cr)-NO <sub>2</sub>	CH <sub>3</sub> CN /EtOH	5	70	67	3	55	8	34
5	MIL-101(Cr)-NO <sub>2</sub>	CH <sub>3</sub> CN	2	70	93	1	79	11	9
6	MIL-101(Cr)-NO <sub>2</sub>	Toluene	3	70	88	2	37	25	36
7	MIL-101(Cr)-NO <sub>2</sub>	CH <sub>3</sub> CN	3	70	82	6	56	22	16
8	MIL-101(Cr)-NO <sub>2</sub>	CH <sub>3</sub> CN	4	70	100	2	82	6	10
9	MIL-101(Cr)-SO <sub>3</sub> H	CH <sub>3</sub> CN	4	70	93	18	67	9	6
10	MIL-101(Cr)-NH <sub>2</sub>	CH <sub>3</sub> CN	4	70	99	30	40	8	22
11	MIL-100(Fe)	CH <sub>3</sub> CN	4	70	99	15	54	14	17
12	UiO-66(Zr)	CH <sub>3</sub> CN	4	70	90	26	19	47	8
13	UiO-66(Zr)-NO <sub>2</sub>	CH <sub>3</sub> CN	4	70	99	17	59	22	2
14	Cu <sub>3</sub> (BTC) <sub>2</sub>	CH <sub>3</sub> CN	4	70	98	31	51	15	3
15	Cr <sub>2</sub> O <sub>3</sub>	CH <sub>3</sub> CN	4	70	95	22	51	23	4
16	Cr(OAc) <sub>3</sub>	CH <sub>3</sub> CN	4	70	96	15	47	30	8
17	-	CH <sub>3</sub> CN	4	70	98	27	44	25	4
18	2-nitroterephthalic acid	CH <sub>3</sub> CN	4	70	100	1	6	1	92
19	MIL-101(Cr)-NO <sub>2</sub> <sup>c</sup>	CH <sub>3</sub> CN	4	70	100	4	69	0	27
20	MIL-101(Cr)-NO <sub>2</sub> <sup>e</sup>	CH <sub>3</sub> CN	4	70	100	0	90	0	10

<sup>a</sup> Reaction condition: **1** (0.5 mmol), **2** (0.55 mmol), catalyst (0.1 mmol of metal), solvent (2 mL).

<sup>b</sup> Determined by GC.

<sup>c</sup> Reaction was performed in the presence of pyridine (0.1 mmol).

---

<sup>e</sup>Reaction was performed in the pure oxygen atmosphere.

As commented earlier, a wide range of Lewis and Brønsted acids have been reported as catalysts for the synthesis of benzimidazole derivatives. Therefore it was of special interest to study the activity of MIL-101(Cr)-SO<sub>3</sub>H that combines the Lewis acidity of Cr metal nodes with the Brønsted acid sites of sulfonic groups. In this context, MIL-101(Cr)-SO<sub>3</sub>H has already been reported as an efficient Brønsted acid catalyst for a series of reactions particularly in biomass valorisation.<sup>60, 61</sup> It was observed that MIL-101(Cr)-SO<sub>3</sub>H exhibits 67% of yield for the reaction of **1** and **2** in acetonitrile at 70 °C after 4 h (entry 9, Table 2). Further, the use of MIL-101(Cr)-NH<sub>2</sub> afforded 40% yield of **4** under similar reaction conditions (entry 10, Table 2). On other hand, the reaction of **1** with **2** using MIL-100(Fe) as catalyst reached 54% yield of **4** under identical reaction conditions (entry 11, Table 2).

To further expand the study on the influence of substituents on the catalytic activity of robust MOFs, UiO-66(Zr) was also tested as catalyst for the condensations between **1** and **2**. The yield of **4** was 19% with UiO-66(Zr) under the optimized reaction conditions (entry 12, Table 2) which is comparatively lower than using MIL-101(Cr)-H and MIL-100(Fe) as catalysts. Interestingly, the yield of product **4** under identical conditions increased to 59% using UiO-66(Zr)-NO<sub>2</sub> as solid catalyst under identical conditions (entry 13, Table 2). These control experiments have clearly demonstrated that under identical reaction conditions the activity of MIL-101(Cr)-H or UiO-66(Zr) is

lower compared to MIL-101(Cr)-NO<sub>2</sub> or UiO-66(Zr)-NO<sub>2</sub> solid catalysts. This higher activity of nitro-functionalized MIL-101(Cr)-NO<sub>2</sub> or UiO-66(Zr)-NO<sub>2</sub> is attributed due to the higher strength of the Lewis acid centres in these catalysts due to the electron-withdrawing effect of -NO<sub>2</sub> group on the aromatic ring. Furthermore, Cu<sub>3</sub>(BTC)<sub>2</sub> was also employed as solid catalyst for this reaction, observing 51% yield of **4** (entry 14, Table 2) under identical conditions.

In order to understand the role of MIL-101(Cr)-NO<sub>2</sub> in this reaction, a series of control experiments were performed and the results are given in Table 2. The use of homogeneous metal salts such as Cr<sub>2</sub>O<sub>3</sub> and Cr(OAc)<sub>3</sub> as catalysts resulted in 51 and 47% yields of **4** under identical conditions (entries 15-16, Table 2). On other hand, the reaction of **1** with **2** under similar conditions in the presence of 2-nitroterephthalic acid afforded 6% yield of the product (entry 18, Table 2). These experiments clearly reveal that the catalytic activity of MIL-101(Cr)-NO<sub>2</sub> originates from the Lewis acidity around the nodal Cr<sup>3+</sup> atoms in MIL-101(Cr)-NO<sub>2</sub>. These results are in agreement with earlier reports in a wide range of reactions.<sup>18, 50</sup> Fig. 2 shows the evolution of yield of **4** from **1** and **2** using MIL-101(Cr)-H and MIL-101(Cr)-NO<sub>2</sub> as catalysts. Furthermore, the activity of MIL-101(Cr)-NO<sub>2</sub> was significantly reduced for the reaction of **1** with **2** upon addition of pyridine as a catalyst poison. This lower activity of MIL-101(Cr)-NO<sub>2</sub> in the presence of pyridine can be explained considering neutralization of Lewis sites (Cr<sup>3+</sup>) by pyridine (entry 19, Table 2).

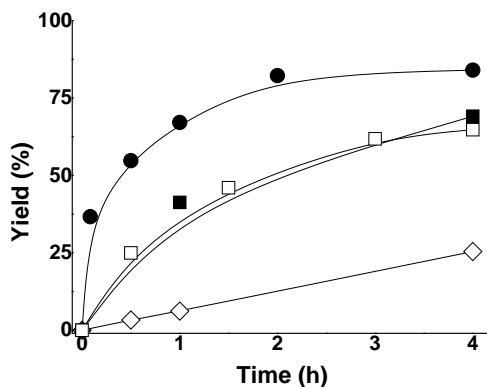


**Fig. 2** Time-yield plot for benzimidazole formation using MIL-101(Cr)-NO<sub>2</sub> (●) or MIL-101(Cr)-H (■) as catalysts. Control experiments using pyridine in the presence (□) or in the absence of MIL-101(Cr)-NO<sub>2</sub> (◇) are also shown. Reaction condition: **1**(0.5 mmol), **2** (0.55 mmol), catalysts (0.1 mmol of metal), CH<sub>3</sub>CN (2mL), 70 °C.

Reusability tests using the most active MIL-101(Cr)-NO<sub>2</sub> catalyst show that the activity decreases from the first to the third catalytic cycle, while, then, the activity is maintained up to the fifth cycle. Importantly, it was observed that the catalyst retains its initial crystallinity upon extensive use as catalyst and SEM analysis of the samples show no changes in the particle morphology (Fig. S13). Furthermore, elemental analysis by ICP-AES of the liquid phase after removal of the solid indicated negligible amount of Cr 0.02 wt%, thus supporting the heterogeneity of the process in the case of MIL-101(Cr)-NO<sub>2</sub>. Combustion elemental analysis of the used MIL-101(Cr)-NO<sub>2</sub> catalyst showed slight increase of the nitrogen content, even though it has been thoroughly washed with CH<sub>3</sub>CN (see experimental section), respect to the fresh sample. This increase of nitrogen content has been attributed to the occurrence of strong adsorption of the basic nitrogen reagents and intermediates on to the acid sites of the MIL-101(Cr)-NO<sub>2</sub> and, therefore, partially blocking the active sites (Table S2).

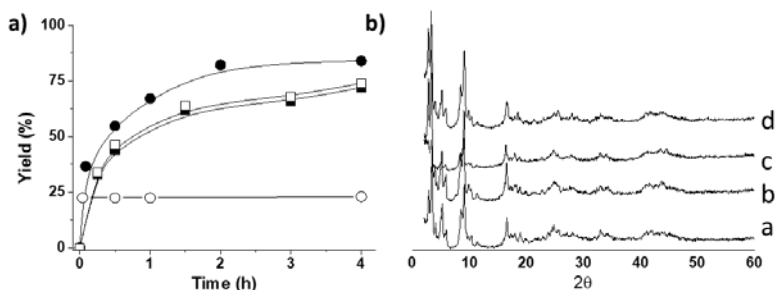


**Fig. 3** a) Reusability of the MIL-101(Cr)-NO<sub>2</sub> for the condensation of **1** with **2** to form the corresponding benzimidazole **4**; b) PXRD of the fresh (a), 1<sup>st</sup> use (b), 3<sup>rd</sup> use (c) and 5<sup>th</sup> use (d) MIL-101(Cr)-NO<sub>2</sub> catalyst. Reaction condition: **1**(0.5 mmol), **2** (0.55 mmol), catalysts (0.1 mmol of metal), CH<sub>3</sub>CN (2mL), 70 °C.

An important issue in heterogeneous catalysis is to confirm that the process is promoted by the active sites on the solid or not by any possible leached metal species present in the solution. To address this point, hot-filtration experiment was performed starting the reaction under the conventional conditions and removing the solid catalyst by filtration at about 50% conversion. Then, the reaction mixture was stirred in the absence of catalyst for the remaining time. The results are presented in Fig. 3. It was observed that the reaction did not progress without the solid catalyst and the product yield remains constant. These data are compatible with the conclusion that the reaction is being promoted exclusively by the active sites of MIL-101(Cr)-NO<sub>2</sub> solid rather than by any leached species.

Table 3 provides a comparison of the catalytic performance of MIL-101(Cr)-NO<sub>2</sub> with some of the catalysts reported in the literature for the synthesis of **4** in terms of solvent, reaction temperature, time and the number of reuses. As it can be seen there, the activity of MIL-

101(Cr)-NO<sub>2</sub> is slightly lower or comparable to other reported catalysts. However, MIL-101(Cr)-NO<sub>2</sub> appears as a stable catalyst at least for five uses. Further, MIL-101(Cr)-NO<sub>2</sub> is one of the few examples in where the solid is used without the requirement of post-synthetic modification.

**Table 3** Comparison of the catalytic activity of MIL-101(Cr)-NO<sub>2</sub> with other catalysts for the synthesis of **4**.

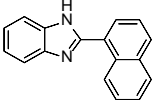
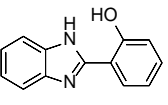
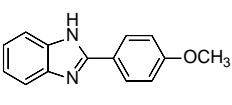
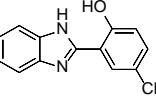
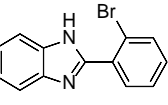
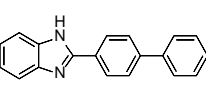
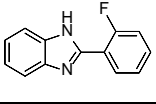
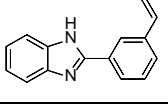
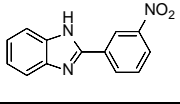
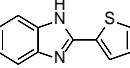
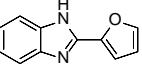
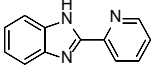
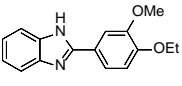
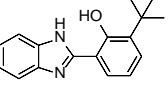
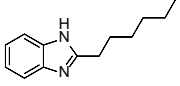
Catalyst	Conditions	Yield (%)	Reuses	Ref.
CuO/SiO <sub>2</sub>	MeOH, RT, 4 h	93	5	[62]
Ag <sub>2</sub> CO <sub>3</sub> /celite	EtOH, 70 °C, 3 h	94	-	[63]
Fe(III)-Schiff base/SBA-15	H <sub>2</sub> O, reflux, 3 h	92	6	[64]
N,N-DMA/graphite (DMA: N,N-dimethylaniline)	EtOH, 75 °C, 3 h	67	3	[65]
CoO	EtOH, RT, 6 h	93	4	[66]
Nano ZnO	EtOH, reflux, 2 h	88	3	[67]
Nano sulphated zirconia	EtOH, 78 °C, 5 h	92	3	[67]
Nano-γ-alumina	EtOH, 75 °C, 5 h	85	3	[67]
Nano ZSM-5	EtOH, 75 °C, 5 h	75	3	[67]
SiO <sub>2</sub> -OSO <sub>3</sub> H	EtOH, 80 °C, 0.5 h	92	3	[68]
UiO-66(Zr)-NH-SO <sub>3</sub> H	EtOH, RT, 1 h	97	5	[33]
TiCl <sub>3</sub> OTf	EtOH, RT, 1.25 h	84	-	[69]
VOSO <sub>4</sub>	EtOH, RT, 1 h	92	4	[70]
MIL-101(Cr)-NO <sub>2</sub>	ACN, 70 °C, 4 h	82	5	This work

After screening different catalysts and various reaction conditions for the synthesis of **4**, the scope of MIL-101(Cr)-NO<sub>2</sub> was explored as heterogeneous solid catalyst for the synthesis of a wide range of benzimidazole derivatives (Table 4). The reaction of 1-naphthylbenzaldehyde with **1** using MIL-101(Cr)-NO<sub>2</sub> as catalyst afforded the corresponding naphthyl benzimidazole derivative in 84% yield. 2-Hydroxy- and 4-methoxybenzaldehydes were reacted successfully with **1** in the presence of MIL-101(Cr)-NO<sub>2</sub> to afford 71 and 78% yields of their corresponding products. On other hand, the

reaction between 2-hydroxy-5-chlorobenzaldehyde and **1** afforded the expected benzimidazole in 60% yield. Furthermore, 4-phenylbenzaldehyde also reacted with **1** to give 54% yield of the corresponding product. These lower yields may be due to the bulkier nature of these aldehydes which may experience some diffusion limitations to reach the active sites. Interestingly, aldehydes bearing electron withdrawing substrates like 2-fluoro-, 2-bromo- and 3-nitrobenzaldehydes reacted with **1** to provide respective benzimidazoles in 80, 71 and 92% yields under the optimized conditions. The enhanced activity of these aldehydes respect to aldehydes with electron donating groups may be due to the rapid formation of the corresponding imine due to the higher reactivity of carbonyl groups with higher positive charge density. Analogously, 3-styrylbenzaldehyde reacted with **1** in the presence of MIL-101(Cr)-NO<sub>2</sub> to give the respective product in 91% yield. This enhanced yield is highly promising since the final heterocyclic product bears vinyl groups which can be readily used as monomers in the synthesis of polymers. Heterocyclic aldehydes like 2-thiophenenecarbaldehyde, 2-furfural and 2-pyridinecarbaldehyde also reacted with **1** using MIL-101(Cr)-NO<sub>2</sub> as catalyst to afford the corresponding benzimidazoles in 72, 64 and 51% yields under identical conditions. These lower yields may be due to the competitive binding of heteroatoms with the Lewis acid sites, but further studies are necessary to prove this hypothesis. 4-Ethoxy-3-methoxybenzaldehyde and 3-t-butyl-2-hydroxybenzaldehydes also gave the respective benzimidazoles in 84 and 70% yields using MIL-101(Cr)-NO<sub>2</sub> as solid catalyst without much diffusion limitations. Finally, the reaction between 1-heptanal and **1**

exhibited 53% yield of the hexylbenzimidazole under identical conditions. This moderate activity may be due to the lower reactivity of aliphatic aldehyde than aromatic aldehydes. These results indicate that MIL-101(Cr)-NO<sub>2</sub> is a general and convenient solid catalyst for the synthesis of wide ranges of benzimidazoles in moderate to high yields.

**Table 4** Structures and the corresponding yields of benzimidazole derivatives prepared using MIL-101(Cr)-NO<sub>2</sub> as a multifunctional solid catalyst.<sup>a</sup>

		
84	71	78
		
60	71	54
		
80	91	92
		
72	64	51
		
84	70	53

<sup>a</sup> Reaction conditions: aldehyde (0.5 mmol), **2** (0.55 mmol), MIL-101(Cr)-NO<sub>2</sub> (0.1 mmol Cr), ACN (2 mL), 70 °C, 4 h.

<sup>b</sup> Determined by GC.



#### 4.4.3 Characterization of the Lewis acid centers

In order to get some understanding of the higher catalytic activity achieved with MIL-101(Cr)-NO<sub>2</sub> as solid Lewis acid catalyst respect to the parent MIL-101(Cr)-H, infrared spectroscopy was employed as a spectroscopic tool for CD<sub>3</sub>CN as a probe molecule to determine the relative Lewis acid sites.<sup>71</sup> Prior to the FT-IR measurements, the solid samples were activated at 150 °C under vacuum for 3 h to remove the water molecules coordinated to the Cr<sup>3+</sup> metal centers.<sup>72, 73</sup> Subsequently, CD<sub>3</sub>CN was supplied to the thermally activated solids. Fig. 4 shows the equilibrated curve corresponding to the adsorption of CD<sub>3</sub>CN on the activated solids. In agreement with previous reports, the characteristic  $\nu(\text{CN})$  and  $\nu(\text{CD}_3)$  vibration bands corresponding to CD<sub>3</sub>CN physisorbed or coordinated to the Cr<sup>3+</sup> Lewis centers can be clearly distinguished.<sup>73</sup> It should be noted that for the FT-IR experiments the same amount of solid was employed, thus, the higher intensity of the band at about 2323 cm<sup>-1</sup> for the MIL-101(Cr)-NO<sub>2</sub> respect to the MIL-101(Cr)-H indicates the higher population of Cr<sup>3+</sup> Lewis centers present in this sample. In addition, the higher  $\nu(\text{CN})$  wavenumber measured for MIL-101(Cr)-NO<sub>2</sub> solid respect to that observed for MIL-101(Cr)-H (2320 cm<sup>-1</sup>) is an indication of the stronger Lewis character of the former sample. Interestingly, the Lewis acidity of the MIL-101(Cr)-NO<sub>2</sub> characterized by the  $\nu(\text{CN})$  at 2323 cm<sup>-1</sup> is higher than that observed for related MIL-100(Fe) or MIL-100(Al) material with analogous metal nodes.<sup>74</sup> It is well-known that the Lewis acidity of Al<sup>3+</sup> ions is higher than that of Cr<sup>3+</sup> ones, while in this case the presence of the nitro group in the terephthalate

organic ligand of the MIL-101(Cr)-NO<sub>2</sub> has a positive effect inducing a stronger acidity on the Cr<sup>3+</sup> metal centers respect to Al<sup>3+</sup> ones. All these observations support that the higher catalytic activity observed for the MIL-101(Cr)-NO<sub>2</sub> solid derives from the increased Lewis acidity around Cr<sup>3+</sup> nodes that enhances both the acid and redox steps in benzimidazole formation.

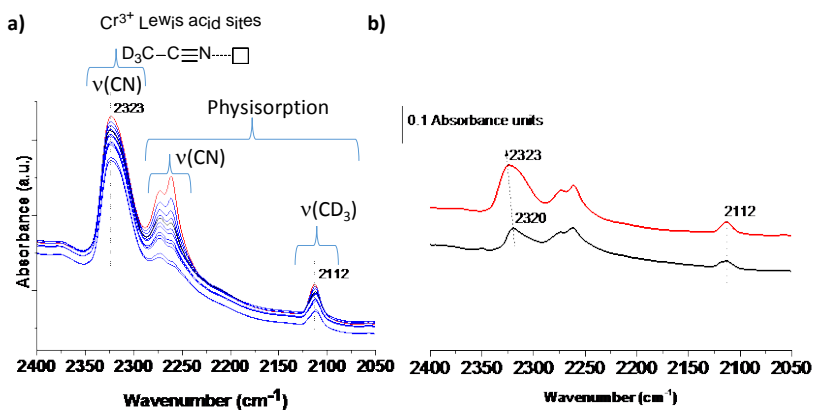


**Fig. 4** a) FT-IR spectra of CD<sub>3</sub>CN adsorbed in MIL-101(Cr)-NO<sub>2</sub> at 6 mbar and -170 °C; Blue line spectra show the CD<sub>3</sub>CN desorption from MIL-101(Cr)-NO<sub>2</sub>. b) Comparison of the FT-IR spectra of CD<sub>3</sub>CN adsorbed on MIL-101(Cr)-NO<sub>2</sub> (red line) or MIL-101(Cr)-H (black line) at 6 mbar and -170 °C.

## 4.5. Conclusions

The results provided here show that the activity and selectivity of MIL-101(Cr)-H for the cyclocondensation of **1** and **2** to give **4** can be improved by nitro substitution on the terephthalate linker resulting in MIL-101(Cr)-NO<sub>2</sub>. The process requires a bifunctional (Lewis acid and oxidation sites) catalyst.<sup>18</sup> Further, MIL-101(Cr)-NO<sub>2</sub> is stable up

to five uses without activity decay as shown by leaching tests to prove the heterogeneity of the reaction. The catalyst exhibited a wide scope respect to the benzaldehyde derivatives to obtain different benzimidazole derivatives. MIL-101(Cr)-NO<sub>2</sub> does not need any post-synthetic treatment, while some of previously reported catalysts require post-synthetic modifications.<sup>33, 34, 59</sup> Overall, the present catalytic data provide additional insights to the existing literature in using MIL-101(Cr)-NO<sub>2</sub> as heterogeneous bifunctional catalyst for the synthesis of nitrogen heterocycles.

## 4.6 Acknowledgements

AD thanks the University Grants Commission, New Delhi, for the award of an Assistant Professorship under its Faculty Recharge Programme. AD also thanks the Department of Science and Technology, India, for the financial support through Extra Mural Research Funding (EMR/2016/006500). Financial support by the Spanish Ministry of Science and Innovation (Severo Ochoa and RTI2018-098237-CO21) and Generalitat Valenciana (Prometeo 2017/083) is gratefully acknowledged. S.N. thanks financial support by the Fundación Ramón Areces (XVIII Concurso Nacional para la Adjudicación de Ayudas a la Investigación en Ciencias de la Vida y de la Materia, 2016), Ministerio de Ciencia, Innovación y Universidades RTI2018-099482-A-I00 project and Generalitat Valenciana grupos de investigación consolidables 2019 (AICO/2019/214) project.

## 4.7 References

1. G. Ferey, C. Mellot-Draznieks, C. Serre, F. Millange, J. Dutour, S. Surble and I. Margiolaki, *Science*, 309 (2005) 2040.
2. L. Bromberg and T.A. Hatton, *ACS Appl. Mater. Interfaces*, 3 (2011) 4756.
3. F.G. Cirujano, A. Leyva-Pérez, A. Corma and F.X. Llabrés i Xamena, *ChemCatChem*, 5 (2013) 538.
4. J. Kim, S.-N. Kim, H.-G. Jang, G. Seo and W.-S. Ahn, *Appl. Catal. A: Gen.*, 453 (2013) 175.
5. B. Li, K. Leng, Y. Zhang, J.J. Dynes, J. Wang, Y. Hu, D. Ma, Z. Shi, L. Zhu, D. Zhang, Y. Sun, M. Chrzanowski and S. Ma, *J. Am. Chem. Soc.*, 137 (2015) 4243.
6. L. Mitchell, B. Gonzalez-Santiago, J.P.S. Mowat, M.E. Gunn, P. Williamson, N. Acerbi, M.L. Clarke and P.A. Wright, *Catal. Sci. Technol.*, 3 (2013) 606.
7. S. Bhattacharjee, C. Chen and W.-S. Ahn, *RSC Adv.*, 4 (2014) 52500.
8. E. Niknam, F. Panahi, F. Daneshgar, F. Bahrami and A. Khalafi-Nezhad, *ACS Omega*, 3 (2018) 17135.
9. L.A. Darunte, A.D. Oetomo, K.S. Walton, D.S. Sholl and C.W. Jones, *ACS Sustainable Chem. Eng.*, 4 (2016) 5761.
10. L. Gao, C.-Y.V. Li, H. Yung and K.-Y. Chan, *Chem. Commun.*, 49 (2013) 10629.
11. M. Hartmann and M. Fischer, *Micropor. Mesopor. Mater.*, 164 (2012) 38.
12. W. Ma, L. Xu, Z. Li, Y. Sun, Y. Bai and H. Liu, *Nanoscale*, 8 (2016) 10908.
13. T. Toyao, M. Fujiwaki, Y. Horiuchi and M. Matsuoka, *RSC Adv.*, 3 (2013) 21582.
14. H. Yu, J. Xie, Y. Zhong, F. Zhang and W. Zhu, *Catal. Commun.*, 29 (2012) 101.
15. L. Ma, L. Xu, H. Jiang and X. Yuan, *RSC Adv.*, 9 (2019) 5692.
16. M. Saikia and L. Saikia, *RSC Adv.*, 6 (2016) 15846.
17. Y.-X. Zhou, Y.-Z. Chen, Y. Hu, G. Huang, S.-H. Yu and H.-L. Jiang, *Chem. Eur. J.*, 20 (2014) 14976.
18. A. Santiago-Portillo, J.F. Blandez, S. Navalón, M. Álvaro and H. García, *Catal. Sci. Technol.*, 7 (2017) 1351.
19. A. Herbst, A. Khutia and C. Janiak, *Inorg. Chem.*, 53 (2014) 7319.
20. A. Kumar, R.A. Maurya and D. Saxena, *Mol. Diversity*, 14 (2010) 331.

21. L.A. Reddy, G.C. Malakondaiah, A.S. Reddy, B.V. Bhaskar, V. Himabindu, A. Bhattacharya and R. Bandichhor, *Org. Process Res. Dev.*, 13 (2009) 1122–1124.
22. Z.-H. Zhang, T.-S. Li and J.-J. Li, *Monat. Chem.*, 138 (2007) 89.
23. M.P. Singh, S. Sasmal, W. Lu and M.N. Chatterjee, *Synthesis*, (2000) 1380.
24. R. Trivedi, S.K. De and R.A. Gibbs, *J. Mol. Catal. A: Chem.*, 245 (2006) 8.
25. K. Nagata, T. Itoh, H. Ishikawa and A. Ohsawa, *Heterocycles*, 61 (2003) 93.
26. H.Q. Ma, Y.L. Wang, J.P. Li and J.Y. Wang, *Heterocycles*, 71 (2007) 135.
27. P. Gogoi and D. Konwar, *Tetrahedron Lett.*, 47 (2006) 79.
28. Y. Kawashita, N. Nakamichi, H. Kawabata and M. Hayashi, *Org. Lett.*, 5 (2003) 3713.
29. A. Dhakshinamoorthy, K. Kanagaraj and K. Pitchumani, *Tetrahedron Lett.*, 52 (2011) 69.
30. G.-F. Chen and X.-Y. Dong, *J. Chem.*, 9 (2012) 289.
31. K. Madasamy, S. Kumaraguru, V. Sankar, S. Mannathan and M. Kathiresan, *New J. Chem.*, 43 (2019) 3793.
32. H. Kaur, M. Venkateswarulu, S. Kumar, V. Krishnan and R.R. Koner, *Dalton Trans.*, 47 (2018) 1488.
33. M. Homae, H. Hamadi, V. Nobakht, M. Javaherian and B. Salahshournia, *Polyhedron*, 165 (2019) 152.
34. R. Kardanpour, S. Tangestaninejad, V. Mirkhani, M. Moghadam, I. Mohammadpoor-Baltork and F. Zadehahmadi, *J. Solid State Chem.*, 235 (2016) 145.
35. J. Canivet, M. Vandichel and D. Farrusseng, *Dalton Trans.*, 45 (2016) 4090.
36. A. Dhakshinamoorthy, A.M. Asiri and H. Garcia, *Chem. Soc. Rev.*, 44 (2015) 1922.
37. S. Yuan, L. Feng, K. Wang, L. Zou, Y. Zhang, J. Li and H.-C. Zhou, *Adv. Mater.*, 30 (2018) 1704303.
38. A. Dhakshinamoorthy and H. Garcia, *ChemSusChem*, 7 (2014) 2392.
39. M.-L. Hu, V. Safarifard, E. Doustkhah, S. Sadegh Rostamnia, A. Morsali, N. Nouruzi, S. Beheshti and K. Akhbari, *Micropor. Mesopor. Mater.*, 256 (2018) 111.
40. Y.-B. Huang, J. Liang, X.-S. Wang and R. Cao, *Coord. Chem. Rev.*, 46 (2017) 126.
41. C. Xu, R. Fang, R. Luque, L. Chen and Y. Li, *Coord. Chem. Rev.*, 388 (2019) 268.

42. D. Azarifar, R. Ghorbani-Vaghei, S. Daliran and A.R. Oveisi, *ChemCatChem*, 9 (2017) 1992.
43. M.R. Ghaleno, M. Ghaffari-Moghaddam, M. Khajeh, A.R. Oveisi and M. Bohlooli, *J. Colloid Interf. Sci.*, 535 (2019) 214.
44. A. Kirchon, L. Feng, H.F. Drake, E.A. Joseph and H.-C. Zhou, *Chem. Soc. Rev.*, 47 (2018) 8611.
45. A. Dhakshinamoorthy, M. Alvaro and H. Garcia, *ChemCatChem*, 2 (2010) 1438.
46. A. Dhakshinamoorthy, M. Alvaro and H. Garcia, *ACS Catal.*, 1 (2011) 836.
47. A. Dhakshinamoorthy, A.M. Asiri and H. Garcia, *Chem. Eur. J.*, 22 (2016) 8012.
48. A. Santiago-Portillo, S. Navalón, M. Álvaro and H. García, *J. Catal.*, 365 (2018) 450.
49. A. Santiago-Portillo, S. Navalon, F. Cirujano, F. Llabrés i Xamena, M. Alvaro and H. Garcia, *ACS Catal.*, 5 (2015) 3216.
50. A. Santiago-Portillo, S. Navalón, P. Concepción, M. Álvaro and H. García, *ChemCatChem*, 9 (2017) 2506.
51. M. Lammert, S. Bernt, F. Vermoortele, D.E. De Vos and N. Stock, *Inorg. Chem.*, 52 (2013) 8521–8528.
52. S. Bernt, V. Guillerme, C. Serre and N. Stock, *Chem. Commun.*, 47 (2011) 2838.
53. B. Li, Y. Zhang, D. Ma, L. Li, G. Li, G. Li, Z. Shi and S. Feng, *Chem. Commun.*, 48 (2012) 6151.
54. M. Kandiah, M.H. Nilsen, S. Usseglio, S. Jakobsen, U. Olsbye, M. Tilset, C. Larabi, E.A. Quadrelli, F. Bonino and K.P. Lillerud, *Chem. Mater.*, (2010) 6632.
55. Y. Bansal and O. Silakari, *Bioorg. Med. Chem.*, 20 (2012) 6208.
56. D. Kumar, D.N. N. Kommi, R. Chebolu, S.K. Garg, R. Kumar and A.K. Chakraborti, *RSC Adv.*, 3 (2013) 91.
57. M. Curini, F. Epifano, F. Montanari, O. Rosati and S. Taccone, *Synlett* (2011) 1832.
58. R. Wang, X. Lu, X. Yu, L. Shi and Y. Sun, *J. Mol. Catal. A: Chem.*, 266 (2007) 198.
59. A. Dhakshinamoorthy, M. Alvaro and H. Garcia, *Catal. Lett.*, 145 (2015) 1600.
60. J. Chen, K. Li, L. Chen, R. Liu, X. Huang and D. Ye, *Green Chem.*, 16 (2014) 2490.
61. A. Herbst and C. Janiak, *CrystEngComm*, 19 (2017) 4092.

62. S.M. Inamdar, V.K. More and S.K. Mandal, *Tetrahedron Lett.*, 54 (2013) 579.
63. E. Soleimani, M.M. Khodaei, H. Yazdani, P. Saei and J. Zavar Reza, *J. Iran. Chem. Soc.*, 12 (2015) 1281.
64. G.R. Bardajee, M. Mohammadi, H. Yari and A. Ghaedi, *Chin. Chem. Lett.*, 27 (2016) 265.
65. H. Sharghi, O. Asemani and S.M.H. Tabaei, *J. Heterocycl. Chem.*, 45 (2008) 1293–1298.
66. M.A. Chari, D. Shobha and T. Sasaki, *Tetrahedron Lett.*, 52 (2011) 5575.
67. A. Teimouri, A.N. Chermahini, H. Salavati and L. Ghorbanian, *J. Mol. Catal. A: Chem.*, 373 (2013) 38.
68. B. Sadeghi and M. Ghasemi Nejad, *J. Chem.*, (2013) 1–5.
69. J. Azizian, P. Torabi and J. Noei, *Tetrahedron Lett.*, 57 (2016) 185–188.
70. C.S. Digwal, U. Yadav, A.P. Sakla, P.S. Ramya, S. Aaghaz and A. Kamal, *Tetrahedron Lett.*, 57 (2016) 4012.
71. A. Vimont, F. Thibault-Starzyk and M. Datur, *Chem. Soc. Rev.*, 39 (2010) 4928.
72. H. Leclerc, A. Vimont, J.-C. Lavalley, M. Daturi, A.D. Wiersum, P.L. Llwellyn, P. Horcajada, G. Férey and C. Serre, *Phys. Chem. Chem. Phys.*, 13 (2011) 11748.
73. A. Vimont, J.-M. Goupil, J.-C. Lavalley, M. Daturi, S. Surblé, C. Serre, F. Millange, G. Férey and N. Audebrand, *J. Am. Chem. Soc.*, 128 (2006) 3218.
74. C. Volkringer, H. Leclerc, J.-C. Lavalley, T. Loiseau, G. Férey, M. Daturi and A. Vimont, *J. Phys. Chem. C*, 116 (2012) 5710–5719.